

SLAC-PUB-118
June 1965

SPECIAL MODELS AND PREDICTIONS FOR PHOTOPRODUCTION ABOVE 1 GEV^{*}

S. D. Drell

Stanford Linear Accelerator Center
Stanford University, Stanford, California

(An invited talk to the International Symposium on Electron and
Photon Interactions at High Energies, Hamburg 8-12 June, 1965)

*Work supported by the U. S. Atomic Energy Commission

In considering models of photoproduction processes at high energies $\gtrsim 1$ Gev, we begin with a discussion of the production of secondary beams of strongly interacting particles. These applications make the least stringent demands upon the theory since we are primarily concerned only with approximate predictions of fluxes of high energy π mesons, K mesons, or even of anti-nucleons which can then serve as projectiles in subsequent experiments. More refined quantitative results are of secondary importance for the beam production analyses and correspondingly we learn less from them about the detailed theoretical nature of the interactions involved.

In the second part of our discussion we turn to more detailed analyses of the low momentum transfer, or peripheral, processes initiated by photons. Finally in part three we consider the central, or high momentum transfer collisions.

I BEAMS

The contributions from five different types of amplitudes must be included in beam production studies. These are illustrated in Fig. 1 and are expected to play the dominant roles in high energy and low momentum transfer processes, when not forbidden by selection rules.

Before discussing a new beam production process for K^0 mesons arising from diagram (c), I will review briefly the present situation with regard to charged pion photoproduction via one pion exchange¹ as in diagram (a) and as illustrated in more detail in Fig. 2.

The assumption of the peripheral calculation is that the amplitude corresponding to this graph should be the predominant one at high photon and pion energies, $k \sim \omega_q \gg \mu$ and at low momentum transfers, or small production angles, $\theta_q \sim \mu/k$. Under these kinematical conditions the impact parameter in the collision can be large, $\sim \frac{1}{2q} = 1$ fermi, since an "almost real" pion is being exchanged between the vertices (a) and (b) in Fig. 2. The corresponding contribution to the cross section is large because the numerator factors evaluated at the pion exchange pole are large themselves, being the product of the pion current at (a) with the total pion absorption cross section at (b).

Experimental support for the approximate validity of this peripheral calculation has been established² for an incident photon beam with maximum energies ranging from 1.2 to 5.8 Gev as shown in the following two graphs in Fig. 3. The factor-of-two agreement near the peak of the angular distribution at $\theta = \mu/\omega_q$ supports the optimism of the peripheral model in its prediction that intense charged pion beams will be produced at electron accelerators at high energies.³ In fact the agreement between the simple model and observation is close enough to motivate further theoretical studies and refinements aimed at accounting for their difference.⁴

Various off mass shell and non-pole-term corrections have been studied and diminish the difference between the model and the data. In particular Itabashi and Hadjioannou found that the static Chew-Low theory applied to 1.2 Gev photoproduction from hydrogen led to a substantial improvement, as illustrated in Fig. 4, and recent work by Stichel and

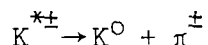
Scholz,⁵ who have included N^* exchange as one possible relativistic extension of this model designed to preserve gauge invariance, leads to a similar increase. The situation is still not clear as we move in from the peak in the distribution at $\theta = \mu/\omega_q$ to the forward angle $\theta = 0^\circ$ because the incident photon must transfer its angular momentum to the nucleon line. We shall return to this point later.

Before doing this, however, one can ask whether the extrapolation from 5 Gev to higher energies, say 20 Gev, can be made with any confidence on the basis of these measurements as well as of the extensive and detailed analyses of experiments with peripheral interactions of strongly interacting particles. With regard to one pion exchange processes at higher energies there is some positive evidence in the recently reported analysis⁶ of peripheral ρ^0 meson production by incident pions of 12 and 18 Gev/c on carbon in the reaction $\pi^- + C \rightarrow \rho^0 + (\text{anything})$. The relevant graph is shown in Fig. 5, and the theoretical inputs are the ρ resonance parameters (energy and decay width) at (a) and the total pion-nucleus cross sections at (b). The correlation of theory with experiment is illustrated in Fig. 6 and again illustrates a factor of two agreement. No major corrections damping this amplitude are observed or anticipated at forward directions due either to reggeization of the pion trajectory or to initial and final state absorption corrections.⁷

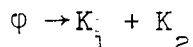
The other candidates for charged pion beam production in Fig. 1 have also been calculated⁸ and only the vector current contribution in graph (d) is found to be a possible major contributor at high energies. However this contribution is significantly smaller than that of the pion current when the ρ exchange amplitude is reduced as found experimentally in the π -nucleon charge exchange analysis.⁹

How is the situation with K meson beams? Here the pole for K meson exchange is approximately $m_K \approx 500$ Mev distant from the physical region and data¹⁰ has not yet been obtained at sufficiently high energies so that relatively this is a small energy interval. Therefore a real quantitative test is still wanting. However the indications at present for photoproduction of K^- at 2.6 and 3.1 Gev from hydrogen are similar to the results found for the pion beam - an approximately correct magnitude ($\approx 4\mu\text{b/ster} - \text{beV/c}$) but an angular distribution that continues to grow instead of decreasing to zero as $\theta \rightarrow 0^\circ$.

For neutral K beams, and in particular for high energy K_2 beams, we turn to the process¹¹ in graph (c) of Fig. 1. There is no charge current for this process as in graph (a) and production of a charged vector K^* followed by the decay

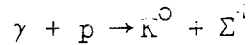


as in (b) and (d) is calculated to be less important. The diffraction production of a ϕ meson in graph (e) with the subsequent decay



is also estimated to be of lesser importance because of the small partial widths for forming the ϕ as well as for its subsequent decay.¹² This leaves the K^* meson as the lightest particle with the quantum numbers of the t or momentum transfer channel and we expect K^* exchange to be a dominant feature in high energy K^0 photoproduction.

In the spirit of making a prediction of the intensity of the K_2 beam emerging from accelerators such as DESY, CEA, Cornell, Erevan, and SLAC the attempt was made to bias calculations to yield a lower limit prediction. In particular only the two body final state in the reaction



is retained as illustrated in Fig. 7 (for example the amplitude to produce a $Y_1^*(1385)$ is ignored altogether). Also the strong damping of this reaction amplitude due to the effect of many open and competing channels is computed with the distorted wave Born approximation method developed primarily by Gottfried and Jackson.¹³

The applicability of this absorption model to vector exchange processes is not well established at high energies. In the 3-4 GeV/c range the K^* exchange mechanism has had good success¹⁴ in fitting the data on the $p\bar{p} \rightarrow \Lambda\bar{\Lambda}$ reaction when the $K^* p\Lambda$ coupling parameters are specified on the basis of SU_3 symmetry in terms of the ρ nucleon coupling and the maximum possible absorption of the low partial waves (no S wave at all) is introduced in the Gottfried-Jackson model again using SU_3 to relate parameters for the $\Lambda\bar{\Lambda}$ and $p\bar{p}$ channels.

Although this gives us some confidence in the model as applied to photoproduction in the 5 GeV energy range, we are also interested in a much higher range of 10 to 20 GeV with a particular eye on SLAC's hopeful future role as a secondary beam factory. It should be recognized that a model such as this which in effect reduces the Born cross section by an

energy independent absorption factor $\eta(b)$

$$\left(\frac{d\sigma}{d\Omega}\right)_{\text{lab}} = \frac{1}{2M_{K^*}^2} \left(\frac{g_{K^*p\Sigma}^2}{4\pi}\right) \left(\frac{g_{K^*K^0\gamma}^2}{4\pi}\right) \frac{\theta^2}{\left[\theta^2 + M_{K^*}^2/k^2\right]^2} \eta(b) \quad (1)$$

$\theta \ll 1 \text{ rad}$
 $k/M_{K^*} \gg 1$

is inadequate asymptotically¹⁵ as $k \rightarrow \infty$. In the approximation of a purely imaginary amplitude for $K^0\Sigma^+$ scattering at high energies s and low momentum transfers t , with the simple parametrization

$$f(s,t) = i \text{Im} f(s,t) = ie^{-\frac{1}{2}A t} \frac{s}{8\pi M_{\Sigma}^2} \sigma_{\text{tot}}(s) \quad (2)$$

the factor $\eta(b)$ is, in the distorted wave Born Approximation, for a collision impact parameter $b = 1/t^{\frac{1}{2}}$

$$\eta(b) = \left\{ 1 - \frac{\sigma_{\text{tot}}(s)}{4\pi A(s)} e^{-b^2/2A(s)} \right\} \quad (3)$$

This factor describes absorption of the K^0 wave along its straight line path through the Σ^+ absorbing potential and is energy independent for constant total cross section σ_{tot} and width $A \approx 10(\text{Bev}^{-2})$ of the diffraction pattern. Hence the peak in the differential cross section (1) continues to grow quadratically with increasing energy, the integrated cross section grows logarithmically, and the absorption factor does nothing to tame the difficult high energy limiting behavior of vector exchange amplitudes that motivated the original application of Regge pole ideas at high energies.

A detailed calculation of the K_2^0 beam has been made¹¹ with the various helicity amplitudes and individual partial waves in the amplitude for the process of Fig. 7 being projected out and reduced by their appropriate absorption factors. In order to establish a lower limit we set $\frac{\sigma_{tot}}{4\pi A} = 1$ corresponding to complete S-wave absorption although the experimental parameters predict a value of $\frac{\sigma_{tot}}{4\pi A} \approx 0.6$.

The $K^{*0}K^0\gamma$ coupling constant is given in terms of the $\rho \rightarrow \pi + \gamma$ radiative decay width, Γ_γ , with the aid of SU_3 symmetry and the assignment of octet transformation properties to the electromagnetic current, by

$$\frac{g_{K^*K\gamma}^2}{4\pi} \approx \frac{1}{8} \Gamma_\gamma$$

As a very conservative estimate we specify $\Gamma_\gamma \sim 0.15$ Mev and our results may be scaled linearly with the radiative decay width as better direct experimental information is obtained. With this choice the radiative decay width of $K_0^{*0} \rightarrow K_0^0 + \gamma$ comes out to be ~ 0.2 Mev. Experimental information on Γ_γ will be discussed in the next section. The intensity of K^0 's computed in this way is illustrated in the following graph (Fig.8) for a 15 Bev incident photon and shows the effect of the final state absorption¹⁶ in reducing the peak beam intensity by a factor of 10. Translating this number to a K_0^0 beam flux consider 4×10^{14} /sec incident 20 Bev electrons producing photons in a $\frac{1}{2}$ radiation length target, as envisaged SLAC operating conditions. If these photons are incident on a 8 grams/cm² hydrogen target they will produce $10^6 K_2^0$'s/sec - Bev/c at 15 Bev within one millirad about $\theta \sim 2^\circ$. This compares favorably to the corresponding flux of K_2^0 's at 0° expected to be produced by an external proton beam with 5×10^{10} protons/sec at CERN or Brookhaven.¹⁷

As an independent comment on the factor of 10 damping in our calculation of K_2 's due to final state absorption we note that at such high energies the vector exchange processes may be more accurately describable in terms of Reggeized trajectories in the spirit of Chew and collaborators. In this case we might be led to modify (1) by a damping factor¹⁸ of

$$\left(\frac{s}{2M_{K^*}M_p} \right)^{2[0.54 - 1.0]} \approx \frac{1}{13}$$

with very similar numerical results. As final word on the K_2 beam we remark that at the 6 Bev energies of CEA and DESY the peak differential cross section is computed to be $\approx 4 \mu\text{b/ster}$, is comparable to the charged K^\pm yields, and should be readily detected.

Of course once we are this far away from the pole, it is a minor additional sin to cast a glance at the nucleon exchange pole and recent results make a few remarks on this topic unmutable. So I ask the forbearance of my theoretical colleagues and remind you that in these considerations it is only the very approximate magnitudes of differential cross sections for small values of the momentum transfer that are of interest to us.

Very recently backward peaks have been observed¹⁹ in π^\pm - proton scattering with cross sections of

$$\begin{aligned} \left(\frac{d\sigma}{d\Omega} \right)_{180^\circ} &\approx 70 \mu\text{b/ster at 4 Gev} \\ \text{cm} &\approx 30 \mu\text{b/ster at 8 Gev} \end{aligned}$$

for the π^+ - proton case. For π^- - proton scattering the backward peaks are smaller by a factor of 5 to 10. If we interpret the π^+ proton scattering in terms of pure one nucleon exchange we find an energy independent result of ≈ 90 mb/ster which is too large by a factor of one to four thousand. However an application of the Gottfried-Jackson model to the nucleon exchange amplitude has been performed recently by Trefil,²⁰ who has reduced the difference between calculation and observation to less than a factor of three and has reproduced approximately the backward angular peaking with the following assumptions:

1) Complete S-wave absorption, corresponding to $\frac{\sigma_T}{4\pi A} = 1$ in Eq. (3).

This number must be $\gtrsim 0.9$ in order to avoid violating the unitarity limit for S-waves. The reduction in cross section due to the absorption is a factor ≈ 100 .

2) Form factors at the π -nucleon vertex and for the nucleon propagator as computed recently by Selleri²¹ for the nucleon removed by ~ 1 Gev from its mass shell. This virtual nucleon effect reduces the cross section by a factor ≈ 25 .

3) Inclusion of N^* exchange which adds coherently with N exchange for the π^+p case and which is the entire story for π^-p scattering. Using similar form factors as for N exchange this adds a contribution of $\sim 40\%$ to the π^+p process and predicts π^-p cross sections about 1/2 the magnitude as for the π^+ case.

The results of Trefil are still largely energy independent and so fail to reproduce the observed drop by a factor of 2-3 in the 4-8 Gev energy range for π^+p scattering. This drop off requires Reggeization of the nucleon trajectory, as for the K^* case.

However now that we are within an order of magnitude agreement, speculations on the anti-proton or baryon beam become fair game. The primary differences between the calculations of

$$\pi + p \rightarrow p + \pi$$

and

$$\gamma + p \rightarrow \bar{p} + (n)$$

are that initial state absorption is missing in the photon induced case. Furthermore according to current conservation the charge part of the electromagnetic vertex times the nucleon propagator has no change in value for the nucleon off the mass shell. Retaining however full reduction of the final state amplitude due to the absorption correction as well as the reduction of the form factor at the pp vertex we can say that an anti-nucleon beam should not be reduced by more than a factor of ≈ 200 below the perturbation predictions. This may not be good theoretical physics but it is still a tremendous anti-nucleon beam - coming to some few microbarns per ster-Bev at 15 BeV. At SLAC operating conditions, this cross section translates into an anti-proton (baryon) beam flux of $\approx 3 \times 10^5$ particles per BeV/c per second into a milli-steradian of solid angle at 15 BeV.

II PERIPHERAL PROCESSES

We turn next to more detailed analyses of the photoproduction of ρ^0 mesons at 0° with the hope of identifying the precise roles of the diffraction and single pion exchange contributions, graphs (b) and (e), in Fig. 1.

It was conjectured that a forward diffraction peak would characterize high energy photoproduction of the zero strangeness neutral vector mesons

since they have quantum numbers in common with the photon. The characteristic predictions of this conjecture are:

- 1) The forward differential cross section $\left(\frac{d\sigma}{d\Omega}\right)_{0^{\circ}} \propto k^2$, i.e. $\left(\frac{d\sigma}{d\Omega}\right)$ increases with the square of the incident photon laboratory energy.
- 2) $\left(\frac{d\sigma}{d\Omega}\right)_{0^{\circ}} \propto A^{4/3}$ - i.e. the amplitude increases with the nuclear surface area where A is the atomic weight.
- 3) $\left(\frac{d\sigma}{d\Omega}\right)$ decreases exponentially with the square of the momentum transfer, i.e. $\propto e^{-a|t|}$, with a half width ≈ 300 Mev as in (2).

All of these predictions are in approximate agreement with the most recent experiments, both with counters and with the bubble chamber²² at CEA. These studies have been carried out in the energy range up to 4.4 Gev with H, C, Al, and Cu as target nuclei and all of the above general features of diffraction scattering were found to be reproduced as reported to this conference. The A dependence of the ρ^0 photoproduction is the same as that found for π -nucleus scattering, following along an approximate $A^{4/3}$ curve for C, Al, and Cu. The energy and angular variations are characteristic of a diffraction mechanism as given above. Moreover the magnitude of the cross sections is very large²³ - in C the forward differential cross section is

$$\left(\frac{d\sigma}{d\Omega}\right)_{\rho^0, 0^{\circ}} = 5 \text{ mb/ster per nucleon at } 4.4 \text{ Gev}$$

and in H

$$\left(\frac{d\sigma}{d\Omega}\right)_{\rho^0, 0^{\circ}} = 1.3 \text{ mb/ster at } 4.4 \text{ Gev}$$

(4)

with the total elastic cross section in hydrogen integrating to

$$\sigma_{\rho^0} = 25 \text{ } \mu\text{b at } 4.4 \text{ Gev.}$$

The theoretical conjecture of diffraction production was accompanied⁸ by a calculation based on the multiperipheral model of Amati, Fubini, and Stanghellini.²⁴ What was computed was the ratio of the $\gamma + p \rightarrow p + \rho^0$ to the $\pi + p \rightarrow \pi + p$ diffraction cross section by replacing the top rungs in the multiperipheral ladder as shown in Fig. 9 with the result

$$\left(\frac{d\sigma}{d\Omega}\right)_{\gamma p} = \left(\frac{1 + \cos^2\theta}{2}\right) \beta_{\rho} \left(\frac{m_{\rho}}{4\Omega\Gamma_{\rho}}\right)^2 \left(\frac{g_{\gamma\pi\omega}^2}{4\pi}\right) \left(\frac{g_{\rho\pi\omega}^2}{4\pi}\right) \left(\frac{d\sigma}{d\Omega}\right)_{\pi N} \quad (5)$$

where β_{ρ} , m_{ρ} , and Γ_{ρ} are the velocity/c, mass, and total decay width of the ρ^0 , respectively; $\left(\frac{d\sigma}{d\Omega}\right)_{\pi N}$ is the π -nucleon diffraction cross section at the same energy and angle, $\left(\frac{g_{\gamma\pi\omega}^2}{4\pi}\right)$ is the dimensionless coupling constant at the $\gamma\pi\omega$ vertex and in terms of the $\omega \rightarrow \pi^0 + \gamma$ radiative decay width is given by

$$\Gamma_{\omega \rightarrow \pi\gamma} = \frac{1}{24} \left(\frac{g_{\gamma\pi\omega}^2}{4\pi}\right) \left(1 - \frac{m_{\pi}^2}{m_{\omega}^2}\right)^3 m_{\omega} \quad (6)$$

and for

$$\Gamma_{\omega \rightarrow \pi\gamma} \sim 1 \text{ Mev, } \frac{g_{\gamma\pi\omega}^2}{4\pi} \approx \frac{1}{30} \quad (7)$$

The coupling constant at the $\rho\pi\omega$ vertex $\frac{g_{\rho\pi\omega}^2}{4\pi}$ has been estimated²⁵ from the measured decay width of ≈ 10 Mev for $\omega^0 \rightarrow 3\pi$, with the assumption that this decay is dominated by $\omega \rightarrow \rho + \pi \rightarrow 3\pi$, to be $g_{\rho\pi\omega}^2/4\pi \approx 12$.

Alternatively we may use (5) to "measure" this constant by comparison with the experimental result (4). This gives $g_{\rho\pi\omega}^2/4\pi = 10$ in very satisfactory agreement with the above theoretical deduction.

Only in hydrogen does an obvious departure from the diffraction mechanism appear in the form of a slower energy variation of the cross section than with k^2 . This is as would be the case if the one pion exchange contribution contributes comparably with the diffraction cross section at the lower energies. These two amplitudes are 90° out of phase and so do not interfere. The one pion exchange contribution decreases with increasing energy as

$$\frac{1}{k^2} \frac{1}{\left[1 + \left(m_\rho^2/2k m_\pi\right)^2\right]^2}$$

in the forward direction and for $k > m_\rho^2/2m_\pi = 2$ Bev approaches

$$\left(\frac{d\sigma}{d\Omega}\right)_{\text{ope}, \rho^0, 0^0} = \frac{3}{8} \left(\frac{g_{\pi NN}^2}{4\pi}\right) \left(\frac{\Gamma_{\rho \rightarrow \pi\gamma}}{m_\rho}\right) \frac{m_\rho^6}{m_\pi^4 M_p^2} \frac{1}{k^2} \quad (8)$$

where $\frac{g_{\pi NN}^2}{4\pi} = 15$ is the π -nucleon coupling constant and $\Gamma_{\rho \rightarrow \pi\gamma}$ is the ρ radiative decay width, analogous to (6) for the ω . If one assumes that the deviation from the diffraction production can be attributed to pion exchange and fits the observed energy variations in this way a value for $\Gamma_{\rho \rightarrow \pi\gamma}$ can be deduced. This analysis has been carried out by Pipkin et.al.,²² with the result $\Gamma_{\rho \rightarrow \pi\gamma} = 1.5 \pm 1.5$ Mev. A similar analysis of ω photoproduction at forward angles leads to the sum of formulas (5) and (8) but with the ω and ρ radiative decay widths interchanged.

Measurement of this functional variation and magnitude of the ω photo-production cross section thus provides a crucial, parameter-free test of this model.

For a number of reasons we have a crucial interest in accurately determining $\Gamma_{\rho \rightarrow \pi\gamma}$ by further photoproduction studies and by direct observation of the radiative decay branching ratio²⁶ or of conversion of a π to a ρ in a Coulomb field.⁸

The first of these is that the K_2 beam prediction discussed earlier is based on a "conservatively" assumed value of $\Gamma_{\rho \rightarrow \pi\gamma} \sim 0.15$ Mev. On purely theoretical grounds there are SU_3 and SU_6 estimates that²⁷

$$\Gamma_{\rho_0 \rightarrow \pi_0 \gamma} = \frac{1}{3} \Gamma_{\omega \rightarrow \pi_0 \gamma} \sim .35 \text{ Mev}$$

or that²⁸

$$\Gamma_{\rho_0 \rightarrow \pi_0 \gamma} = \frac{1}{9} \Gamma_{\omega \rightarrow \pi_0 \gamma} \sim .1 \text{ Mev}$$

and Bronzan and Low²⁹ have conjectured that the ratio of ρ_0 to ω radiative decay widths will be small on the basis of A parity.

Recently it has been proposed³⁰ that one can understand the static magnetic moment of the deuteron in the context of a potential model of the deuteron binding and wave function which meets all other known binding and scattering parameters if exchange current corrections to the impulse approximation calculations are included. In particular with the desired D wave probability $P_D = 0.07$ for the deuteron, the moment in the impulse approximation is

$$\mu_D = (\mu_p + \mu_N) - \frac{3}{2} P_D (\mu_p + \mu_N - \frac{1}{2}) \quad (9)$$

and is too small by 2%. To remove this discrepancy within the context of the impulse approximation requires reducing the D wave probability to less than 4%. The alternative solution to this dilemma is provided by a $\gamma\pi$ exchange current as illustrated in Fig. 10. This is a unique candidate of less than nucleon mass to remedy the moment discrepancy since the deuteron has isotopic spin zero and so only an isotopic scalar current can contribute. Detailed analysis shows that a radiative decay width of $\Gamma_{\rho\pi\gamma} \sim \frac{1}{2} - 1$ Mev supplies the needed addition to the static magnetic moment.³⁰ New evidence in support of this exchange current contribution was presented to this conference in the analysis by Buchanan and Yearian of elastic electron deuteron scattering.³¹ They have measured large angle magnetic scattering cross sections that lie more than 50% above the impulse approximation calculations at momentum transfers of $q \sim 3(\text{fermi})^{-1}$. The exchange current which supplied the needed static magnetic moment correction of 2% contributes the desired large correction, > 50% at $q \sim 3(\text{fermi})^{-1}$ because the form factor associated with this contribution is much tighter and does not fall off as rapidly with increasing q since an exchange operator gives heavier weighting to the region of small interparticle separations.

A final crucial interest in the radiative decay modes of the vector mesons stems from the need to compute their contributions to the large angle pair production cross sections which are being measured as tests of quantum electrodynamics at high momentum transfers. Symmetric μ^{\pm} pair and e^{\pm} pair experiments have been performed³² at CEA and indications of a deviation from the Bethe Heitler formula have been observed in the latter case as published by Blumenthal et.al. and reported to this conference in

Session VI by Professor F. Pipkin. We may review critically at this point the possible corrections due to strong interactions that might lead to any such deviations via virtual Compton terms of the type illustrated in Fig. 11. Recall that for symmetric pairs these terms do not interfere with the Bethe-Heitler ones and so only ratios of virtual Compton to Bethe-Heitler cross-sections are involved. First we compute the background due to the total photoproduction cross section neglecting the fact that the virtual photon producing the lepton pair is off its mass shell. Here we can appeal to the Kramers Kronig relation for forward scattering of light to express the amplitude in terms of the total photo absorption cross section measured at CEA to be $\lesssim 100 \mu\text{b}$ and essentially constant from 1-5 Gev i.e. we insert ($\alpha = 1/137$)

$$A(\omega, 0^0) = -\frac{\alpha}{M} + \frac{i\omega}{4\pi} \sigma_{\text{tot}}(\omega) + \frac{\omega^2}{2\pi^2} P \int_0^{\infty} \frac{d\omega'}{\omega'^2 - \omega^2} \sigma_{\text{tot}}(\omega') \quad (10)$$

The contribution of the absorptive part dominates and leads to the correction factor, R to the Bethe Heitler formula for symmetric pairs³³

$$R = \left\{ 1 + \left(\frac{\omega^2 \sigma_{\text{tot}}}{8\pi\alpha} \right)^2 \tan^4 \theta/2 \right\} \quad (11)$$

where ω is the photon energy and the electron and positron, or μ^- and μ^+ , emerge each with energy $\frac{1}{2} \omega$ and at an angle θ to the left and right of the incident direction. At the highest energies and largest angles of the electron pair experiments at CEA ($\omega \sim 5.5$ Bev at $\theta \sim 7.5^\circ$) this factor corrects the Bethe Heitler formula by $2\frac{1}{2}\%$. However when one recalls the

sharp dip in the cross section at the symmetric point where the transverse current vanishes as illustrated in Fig. 12 and integrates over the experimental resolution which includes much of the bump on either side of the dip, this correction drops effectively to $< 0.2\%$. A similar conclusion applies to the μ pair experiment which extended out to $\theta \sim 10^\circ$ with $\omega = 5$ Bev.

We turn then to contributions of the virtual vector mesons and in particular to the ρ_0 which appears to play the predominant role.³⁴ In terms of the branching ratio for the ρ^0 to decay to an e^-e^+ pair³⁵

$$\frac{\Gamma_{\rho \rightarrow e\bar{e}}}{\Gamma_{\rho}} \lesssim 10^{-4} \quad (12)$$

we can write the differential cross section for symmetric pairs to be produced via a virtual ρ^0

$$\frac{d^3\sigma}{d\theta d\Omega_+ d\Omega_-} = \frac{3}{8\pi^2} \frac{\Gamma_{\rho \rightarrow e\bar{e}}}{m_{\rho}} \frac{k}{m_{\rho}^2} \frac{1}{(1 - s/m_{\rho}^2)^2 + (\Gamma_{\rho}/m_{\rho})^2} \left(\frac{d\sigma}{d\Omega}\right)_{\rho^0, 0^0} \quad (13)$$

where k is the incident photon energy and s is the square of the mass of the pair that is produced; in writing (13) we assume we are near the ρ mass, $s \approx m_{\rho}^2$, and neglect numerator terms $\propto (1 - s/m_{\rho}^2)$. The value for $\left(\frac{d\sigma}{d\Omega}\right)_{\rho^0, 0^0}$ can be taken directly from experiment or expressed via (5) and (6) in terms of the diffraction model. We are interested in the ratio of (13) to the Bethe Heitler contribution which has the simple approximate form for the symmetric case

$$\frac{d^3\sigma}{d\theta d\Omega_+ d\Omega_-} = \frac{\alpha^3}{16\pi^2 k^3} \frac{\cos^2\theta/2}{\sin^6\theta/2} \quad (14)$$

For the largest angles and highest energies in the electron pair experiments this ratio reaches to 0.1 but the effective correction is only 1% when the experimental resolution over the dip in the Bethe Heitler formula is included. Although the observed photo absorption cross sections fail to provide the explanation for the deviation in large angle e^-e^+ pairs from quantum electrodynamic predictions, they may begin to play a substantial role at the extreme points of the muon pair experiment which reaches to a higher value of the mass of the pairs $\sim m_\rho^2$ and, depending on the experimental resolutions, contribute significantly.³⁶

In concluding this section we call attention to a particular interest in detecting and studying the charged pion production cross sections at the precisely forward angle $\theta = 0^0$. The peripheral production processes all lead to peaks at $\theta \sim m/\omega_q$, where ω_q is the energy of the high energy pion emerging at angle θ and m is the mass of the particle exchanged in the t channel with the target nucleons, and within this angle the cross section dips toward zero,³⁷ decreasing as θ^2 . This forward decrease results from the impossibility of conserving the spin angular momentum of the incident transverse photon for a spin zero pion emerging at 0^0 unless the amplitude is accompanied by nucleon spin flip. For single particle exchanges this spin flip occurs with an amplitude proportional to the momentum transferred to the nucleon, which has a minimum value in the forward direction of

$$\left| t_{\text{Min}} \right|^{1/2} \approx \mu^2 \frac{\Delta E}{k} + (\mu^2/2k)^2 \ll \mu^2$$

where k is the incident photon energy and $\Delta E = k - \omega$ the energy transferred to the nucleon in producing the pion with mass μ and energy ω if vector or

spin zero mesons are exchanged in the t channel. Non peripheral processes escape this suppression since there are large matrix elements for spin flip into and/or out of high energy intermediate nucleon states as in Fig. 13. This is also true of peripheral production of pseudoscalar mesons via an axial vector exchange since the nucleon matrix element then has the familiar Gamow-Teller form of β -decay and the amplitude may be written $\langle \vec{\sigma} \rangle \cdot \vec{\epsilon}_\gamma$. The very forward angles of pion (or K meson) photoproduction at high energies thus are very interesting, though difficult, for experimental study since they probe the non peripheral features of the production amplitude as well as a possible exchange of axial mesons which we are tempted to associate with the structure of the axial current in the same way as the ρ , ω , and ϕ enter the vector current structure and knowledge of both energy variations and branching ratios will be of great value.

III CENTRAL COLLISIONS

We also avoid the peripheral plateau by looking at large angle or momentum transfer events. In these central collisions it is possible to test symmetry schemes without major corrections due to mass splittings between different particles assigned to the same multiplets; i.e. under conditions such that $|t|$ and $s \gg \Delta M^2$. Such tests have been proposed by Levinson, Lipkin, and Meshkov³⁹ for the octet model in the SU_3 symmetry group. In meson nucleon scattering these include the equalities.

$$\begin{aligned}
 d\sigma(K^- p \rightarrow \pi^+ \Sigma^-) &= d\sigma(K^- p \rightarrow K^0 \Xi^0) \\
 d\sigma(\pi^- p \rightarrow K^+ \Sigma^-) &= d\sigma(K^- N \rightarrow K^0 \Xi^-) \\
 d\sigma(\pi^- p \rightarrow \pi^+ N_{3/2}^{*-} (1238)) &= 3d\sigma(\pi^- p \rightarrow K^+ Y_1^{*-} (1385))
 \end{aligned} \tag{15}$$

In general, simple equalities such as (15) do not emerge from the unitary symmetry model alone since there are a number of open channels through which the reaction can proceed and their relative phases and magnitudes require the input of dynamical assumptions. Formally, this is stated in the observation that both meson and baryon form octet representations in SU_3 and their product can form 1 , 8 , $8'$, 10 , $\overline{10}$, and 27 dimensional representations. The reaction can thus proceed through any of six channels and their relative amplitudes together with five relative phase factors at any energy determine the branching ratios. Therefore, analyses of these two-body reactions have heretofore contributed little to our confidence in SU_3 which derives largely from the great success in classification of multiplets and in predicting mass splittings within the individual multiplets. Moreover, the intensity of incident meson beams at high energies has been limited so that only a negligible number of events are observed in the laboratory under the condition of large t as desired to avoid large distortions due to mass splittings and kinematic factors from the exact SU_3 as a symmetry in high-energy scattering processes.

Turning to photon initiated reactions $\gamma + \text{Nucleon} \rightarrow \text{Meson} + \text{Baryon}$ we call attention to the important practical fact that a very intense current of electrons, and in particular of 20 Bev electrons as anticipated at SLAC when operative, leads to a photon flux of sufficiently high intensity to more than compensate for the appearance of a fine structure constant $\alpha = \frac{1}{137}$ in the ratio of the photon to meson cross sections. We must first determine the transformation properties of the electromagnetic current in the unitary symmetry scheme. We can then analyze whether two body reactions of this type can provide useful information or checks on the symmetry scheme.

In Lagrangian models of the SU_3 symmetry scheme for elementary particles, it is most natural to introduce the electromagnetic current as a unitary octet. However, it is also possible for the electromagnetic current to have a unitary-singlet component and independent evidence on the transformation properties of the current is desired. The following relations between magnetic moments and between transition amplitudes have been proposed⁴⁰ as tests of the assumption that the electromagnetic current is a pure octet and a U-spin scalar

$$\mu_N = 2\mu_\Lambda \tag{16}$$

$$\langle \rho^0 | \eta\gamma \rangle = \sqrt{3} \langle \rho^+ | \pi^+\gamma \rangle$$

In calculating matrix elements, this is equivalent to equating a photon to the neutral member of the isotopic triplet, ρ^0 , and to the isotopic singlet, ϕ , in the vector meson octet according to the relation.

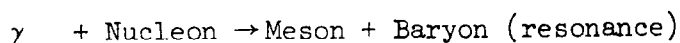
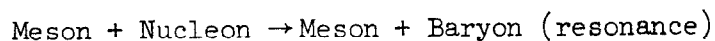
$$|\gamma\rangle = \left\{ |\rho^0\rangle + \frac{1}{\sqrt{3}} |\phi\rangle \right\} \tag{17}$$

I would now like to point out that if the role of SU_3 is quantitatively supported by reactions (15) at high energy and the identification of the photon as in (17) established by processes(16) we can propose a feasible program for testing the validity of the statistical model in high-energy collisions.⁴¹ The idea presented here is to check the very general premise of the statistical model that all open channels should contribute with equal probabilities and with random relative phases, independent of more detailed dynamical questions of specific energy or angle variation of the cross sections.

It is in the central collisions with large s and t that we anticipate the possibility that the concepts of the statistical model may find their natural application. As in the low-energy nuclear physics domain (aside from the direct interaction processes) the colliding particles may be envisioned as forming a compound system with many channels leading to the various possible final state configurations. Aside from phase space and other kinematic factors, the various open reaction channels should be excited with equal probabilities and random relative phases in a statistical model.

This is the very basic general assumption underlying a statistical model. The statistical model has other characteristic predictions with regard to energy and angle variations of elastic cross sections and of multiplicities, in addition, for inelastic ones. These features, however, are tied to various models and "plausible" dynamical assumptions. Recently arguments have been put forward by Bethe and by Woo⁴² pointing out the difficulty of reconciling the observed precipitous drop with energy of the large angle component of the elastic cross section with the statistical model. It is at present not at all clear whether or not the experimental data should be interpreted as indicating the presence of a statistical component in high-energy collisions.

The two-body reactions involving incident meson or photon beams



can proceed through many channels of different angular momenta that control the angular and energy behaviour of cross sections, and of channels with

different internal symmetry quantum numbers that determine the branching ratios for the production of final baryons and mesons with different charge or hypercharge quantum numbers. It is upon these branching ratios that we wish to focus attention. When these cross sections at large s and t are averaged over energy and momentum transfer intervals large compared with the mass splittings within the individual multiplets ($\Delta t^{\frac{1}{2}}, \Delta s^{\frac{1}{2}} > \Delta M$), the branching ratios should be determined solely by the combination coefficients, i.e., the appropriate Clebsch-Gordan coefficients - to form the different SU_3 channels. That each SU_3 channel contributes with equal amplitude and random phase is the very basic and the sole feature of the statistical model on which we base our predictions.

Some of the practical results of these considerations for photons are summarized in the following two tables. The parameter α appears as a mixing parameter for the two independent channels of a meson-nucleon system that transform as an octet. Denoting the corresponding states by $|8\rangle$, to which we assign the meson and nucleon octets, and $|8'\rangle$, respectively, we form the linear combinations

$$\begin{aligned} |8_1\rangle &= \cos \alpha |8\rangle - \sin \alpha |8'\rangle \\ |8_2\rangle &= \sin \alpha |8\rangle + \cos \alpha |8'\rangle \end{aligned}$$

The rotation angle α is defined by the condition of orthogonality

$$\langle 8_1 | 8_2 \rangle = 0$$

and $\alpha = 0$ if the additional symmetry of R invariance⁴³ is invoked. Whereas the consequences of R symmetry are unwelcome at low energies it is possible that R may emerge as an approximate symmetry operation at high energies.

If the special relations between cross sections that are independent of α are verified by experiment and confirm the role of the statistical assumption in high energy central collisions, it will be possible to determine α from the general ratios.

Table I

$\gamma P \rightarrow \pi^+ N$	$34/225 + 19/225$	$\sin^2 2\alpha - 2\sqrt{5}/225$	$\sin 4\alpha$
$\rightarrow \pi^0 P$	$139/450 + 19/450$	$\sin^2 2\alpha - \sqrt{5}/225$	$\sin 4\alpha$
$\rightarrow K^+ \Sigma^0$	$139/450 - 11/450$	$\sin^2 2\alpha + 2\sqrt{5}/225$	$\sin 4\alpha$
$\rightarrow K^0 \Sigma^+$	$34/225 - 11/225$	$\sin^2 2\alpha + 4\sqrt{5}/225$	$\sin 4\alpha$
$\rightarrow K^+ \Lambda$	$31/150 + 1/150$	$\sin^2 2\alpha - \sqrt{5}/75$	$\sin 4\alpha$
$\rightarrow \eta P$	$31/150 - 3/50$	$\sin^2 2\alpha$	

$$\frac{2 [\gamma P \rightarrow K^+ \Sigma^0] - [\gamma P \rightarrow K^0 \Sigma^+]}{2 [\gamma P \rightarrow \pi^0 P] - [\gamma P \rightarrow \pi^+ N]} = 1$$

$$\frac{3 [\gamma P \rightarrow \pi^0 P] - [\gamma P \rightarrow K^+ \Lambda] + 2 [\gamma P \rightarrow \eta P]}{2 [\gamma P \rightarrow \pi^0 P] - [\gamma P \rightarrow \pi^+ N]} = 17/7$$

Table II

$$\begin{aligned}
 \gamma P \rightarrow \pi^+ N_{3/2}^{*0} & \quad 7/50 + 4/225 \sin^2 2\alpha + \sqrt{5}/225 \sin 4\alpha \\
 \rightarrow \pi^0 N_{3/2}^{*+} & \quad 41/1200 + 8/225 \sin^2 2\alpha + 2\sqrt{5}/225 \sin 4\alpha \\
 \rightarrow \pi^- N_{3/2}^{*++} & \quad 49/200 + 4/75 \sin^2 2\alpha + \sqrt{5}/75 \sin 4\alpha \\
 \rightarrow K^+ Y_1^{*0} & \quad 7/100 + 2/225 \sin^2 2\alpha + \sqrt{5}/450 \sin 4\alpha \\
 \rightarrow K^0 Y_1^{*+} & \quad 169/600 + 4/225 \sin^2 2\alpha + \sqrt{5}/225 \sin 4\alpha \\
 \rightarrow \eta N_{3/2}^{*+} & \quad 11/48
 \end{aligned}$$

$$\frac{2 \left[\gamma P \rightarrow \pi^+ N_{3/2}^{*0} \right] - \left[\gamma P \rightarrow \pi^0 N_{3/2}^{*+} \right]}{\left[\gamma P \rightarrow K^0 Y_1^{*+} \right] - 2 \left[\gamma P \rightarrow K^+ Y_1^{*0} \right]} = 59/34$$

$$\frac{\left[\gamma P \rightarrow \pi^+ N_{3/2}^{*0} \right] + \left[\gamma P \rightarrow \pi^0 N_{3/2}^{*+} \right] - \left[\gamma P \rightarrow \pi^- N_{3/2}^{*++} \right]}{\left[\gamma P \rightarrow \pi^0 N_{3/2}^{*+} \right] - 2 \left[\gamma P \rightarrow \pi^+ N_{3/2}^{*0} \right]} = 17/59$$

LIST OF REFERENCES

1. S. D. Drell, Phys. Rev. Letters 5, 278 (1960).
2. R. Blumenthal et al., Phys. Rev. Letters 11, 496 (1963).
W. Blanpied et al., Phys. Rev. Letters 11, 477 (1963) and report to this conference by V. W. Hugnes.
J. Kilner, R. Diebold, and R. L. Walker, Phys. Rev. Letters 5, 518 (1960).
3. J. S. Ballam, 1960 Summer Study (M-200), Hansen Labs of Physics, Stanford University.
S. D. Drell, Rev. Mod. Phys. 33, 458 (1961).
4. K. Itabashi, Phys. Rev. 123, 2157 (1961).
F. Hadjioannou, CERN Report 1962, and Ph.D. Thesis, Physics Department, Stanford University (1961) [quoted in (3)].
M. Thiebaut, Jr., Phys. Rev. Letters 13, 29 (1964).
L. Lakerashvili and S. Mitinyan, Soviet Physics JETP 14, 195 (1962).
For nuclear targets see also J. S. Bell, Phys. Rev. Letters 13, No. 2 (1964).
5. P. Stichel and M. Scholz, Nuovo Cimento X, 34, 138 (1964). Other models may be designed to lead to no increase. It is also very dangerous to have simple Feynman propagators for particles of spin greater than zero appearing in amplitudes for high-energy processes as they may lead to incorrect asymptotic behaviors.
6. L. Jones, Phys. Rev. Letters 14, 186 (1965).
7. See discussion following Eq. (1) and in footnote 16.
8. S. M. Berman and S. D. Drell, Phys. Rev. 133, B791 (1964). U. Maor, Phys. Rev. 135, B1205 (1964).
9. V. Barger and M. Ebel, Wisconsin preprint C 00-30-98 (to be published).

10. J. S. Greenberg et al., Phys. Rev. Letters 14, 741 (1965), and private communications by V. W. Hughes.
11. S. D. Drell and M. Jacob, Phys. Rev. 138, B1312 (1965).
12. These are known to be $\Gamma_{\phi \rightarrow \pi^0} < 0.3 \text{ MeV}$ and $\Gamma_{\phi \rightarrow K_1 K_2} < 2 \text{ MeV}$ and so lead to small diffraction production amplitudes in the calculations of Ref. 8.
13. K. Gottfried and J. Jackson, Nuovo Cimento 34, 735 (1964).
14. G. Cohen and H. Navelet, Saclay preprint (1964) (to be published).
15. See also the discussion of H. Hogaasen and J. Hogaasen, CERN preprint (1965) (to be published).
16. At the peak for K^* exchange, $\theta = M_{K^*}/k$ and the impact parameter in Eq. (3) is $b_{\text{max}} = M_{K^*}^{-1}$ leading to an absorption reduction

$$\eta_{\text{max}}(M_{K^*}^{-1}) = 1 - e^{-\frac{1}{16}} \sim \frac{1}{16}$$

This has the effect of shifting the peak of the K_0 angular distribution to smaller angles where the differential cross section reaches $\frac{1}{10}$ of the value of the peak in the Born approximation. For one-pion exchange cross sections, the impact parameter at the peak $\theta = \mu/k$ is $b = \mu$ and

$$\eta(\mu^{-1}) \approx 1 - e^{-2} \sim 0.9$$

so that the effect of maximal Gottfried-Jackson absorption on the peak differential cross section is very small for one-pion exchange processes.

17. D. Dekkers et al., Report to the Sienna Conference (1963).
J. W. Cronin, in BNL 7957 (May 1964).

18. R.J.N. Phillips and W. Rarita, UCRL 16033 (1965) (to be published).
 In his report, Prof. van Hove has already noted the similar decrease with p_{lab}^{-1} of cross sections dominated by exchange of vector ρ mesons in the t channel. Such a factor applied to the calculated K_2 beam flux would reduce our estimate of $10^6/\text{sec}$ to $2 - 3 \times 10^5/\text{sec}$ and would not alter our primary conclusion.
19. Private communication, W. Krisch to M. Perl. See invited talk of L. van Hove.
20. J. Trefil, work in progress at Stanford.
21. F. Selleri, Cornell preprint.
22. F. Pipkin, private communication, and J. Russell, report to this conference.
 A. H. Rogers, Jr., MIT Physics Department thesis (1965).
23. These absolute cross sections are taken from the work of Pipkin and collaborators. (See report of J. J. Russell to Session 1B.)
24. D. Amati, S. Fubini, and A. Stanghellini, Nuovo Cimento 5, 896 (1962).
25. R. F. Dashen and D. H. Sharp, Phys. Rev. 133, B1585 (1964).
26. G. Fidecaro, private communication (in progress).
27. S. Okubo, Phys. Letters 4, 14 (1963).
28. S. Badier and C. Bouchiat, ORSAY preprint (1965).
 W. E. Thirring, Vienna preprint.
29. J. Bronzan and F. Low, Phys. Rev. Letters 12, 522 (1964).
30. R. J. Adler and S. D. Drell, Phys. Rev. Letters 13, 349 (1964).
 R. J. Adler, Ph.D. thesis, Stanford Physics Department (1964) and SLAC report.
31. M. Yearian, report to Session 1A. We emphasize, as stated in Eq. (30), that this exchange current interaction is just one of a number of

corrections to the impulse approximation current for Pauli particles that are of the same order in the nucleons' $(v/c)^2$. In including it here we are recognizing that a $\rho \rightarrow \pi + \gamma$ radiative decay has a necessary contribution to the magnetic interaction of a deuteron. Its role as a point coupling at $q \gg 0.7M = 3f^{-1}$ is much more dubious theoretically and indeed in conflict with data. Professor E. Loman has just reported that he and Prof. H. Feshbach at MIT have constructed a deuteron model with just under 5% D-state. According to this model, a somewhat smaller $\Gamma_{\rho \rightarrow \pi\gamma}$ would be needed to explain the static magnetic moment (with a detailed integration of the exchange operator over the wave function necessary before we can say just how much).

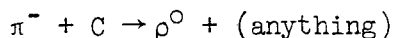
32. J. dePachter, et al., Phys. Rev. Letters 12, 739 (1965).
R. Blumenthal et al., Phys. Rev. Letters 14, 660 (1965).
33. This formula is obtained by introducing Eq. (10) into the calculations in: J. Bjorken, S. Drell, and S. Frautschi, Phys. Rev. 112, 1409 (1958).
34. ω^0 photoproduction at forward angles from hydrogen at 4.4 GeV appears to be reduced by a factor of $\approx 1/6 - 1/8$ relative to ρ^0 's (F. Pipkin, private communication). If this ratio is transcribed via the diffraction model, Eqs. (5) and (6) to a ratio of radiative decay widths, we find from Eq. (7) that $\Gamma_{\rho \rightarrow \pi\gamma} \sim 0.15$ MeV in agreement with the value introduced into the K_2 beam production calculation but smaller by a factor of ~ 3 than that desired in the deuteron-exchange magnetic moment analysis.
35. Zdanis, Madansky, Kraemer, and Hertzbach, Phys. Rev. Letters 14, 721 (1965).
36. A. Krass, Phys. Rev. 138, B1268 (1965), has made some detailed calculations of possible corrections but with more emphasis on the one-pion

exchange contributions as the large diffraction production was not known at the time of this work. The large vector meson photoproduction cross sections also may mean sizable contributions to the very asymmetric μ pairs [S. D. Drell, Phys. Rev. Letters 13, 257 (1964)], and this point is presently under further study (R. Parsons).

37. U. Maor, Phys. Rev. 135, B1205 (1964).
38. See invited paper by L. Osborne to this conference.
39. C. A. Levinson, H. J. Lipkin, and S. Meshkov, Phys. Letters 1, 44 (1962);
Phys. Rev. Letters 10, 361 (1963).
40. S. Okubo, Phys. Letters 4, 14 (1963).
41. This discussion parallels that in a forthcoming paper that discusses both photon and meson initiated reactions according to the statistical model by S. D. Drell, D. Speiser, and J. Weyers.
42. H. A. Bethe, Nuovo Cimento 33, 1167 (1964);
C-H Woo, Phys. Rev. 137, B449 (1965).
43. See for example M. Gell-Mann and Y. Ne'eman, The Eightfold Way (Benjamin and Co., New York, 1964).

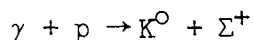
FIGURE CAPTIONS

1. Amplitudes for photoproduction of meson beams.
2. One pion exchange contribution to photoproduction of a charged pion beam.
3. Comparison of experimental results for π^- photoproduction from beryllium with predictions of the one pion exchange calculation [taken from R. Blumenthal et al. (Ref. 2)].
4. Comparison of calculations on $\gamma + p \rightarrow p + \pi^+ + \pi^-$ with experiment at 1.23 GeV.
5. One pion exchange contribution to pion production of a ρ meson.
6. Comparison of experimental results for



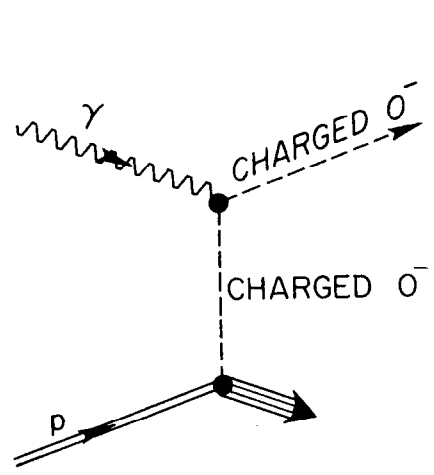
with predictions of the one pion exchange calculations [taken from L. Jones (Ref. 6)].

7. K^* exchange contribution to photoproduction of a K^0 beam in the reaction

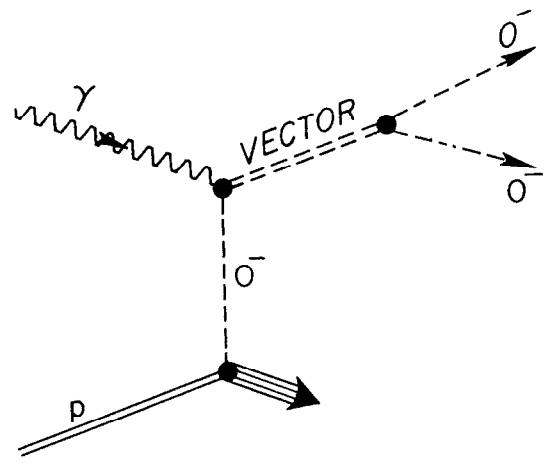


8. Laboratory differential cross section at 15 BeV. Curve (1) gives the Born approximation. Curve (2) is obtained after subtraction of the $j = 1/2$ partial wave. Curves (3) and (4) are respectively obtained after the $j = 1/2, 3/2, 5/2, 7/2$, and all partial waves have been corrected for absorption in the final state [curve taken from (Ref. 11)].
9. Graphs for multiperipheral ladders contributing to pion-nucleon diffraction scattering and to diffraction photoproduction of a ρ^0 .

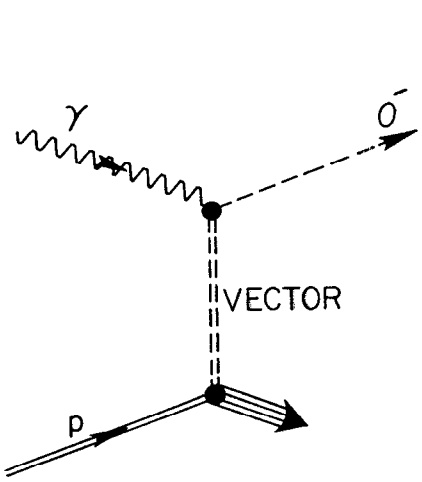
10. $\gamma p \pi$ exchange current contributing to the deuteron magnetic moment and to elastic electron-deuteron scattering; (a) shows a pion-exchange current that vanishes since the deuteron has isotopic spin zero; (b) shows a contribution to the isoscalar nucleon form factor which is included in the impulse approximation.
11. Virtual Compton terms leading to lepton pair (e^-e^+ or $\mu^-\mu^+$) production.
12. Example of dip in Bethe-Heitler formula at the symmetric point plotted as a function of angle of azimuthal deviation for equal energies and polar angles. From Harvard Ph.D. thesis of R. Blumenthal. See Ref. 32.
13. Non-peripheral contribution to photo-pion production.



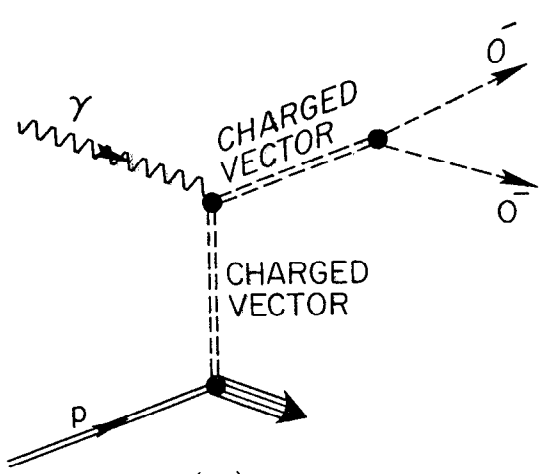
(a)



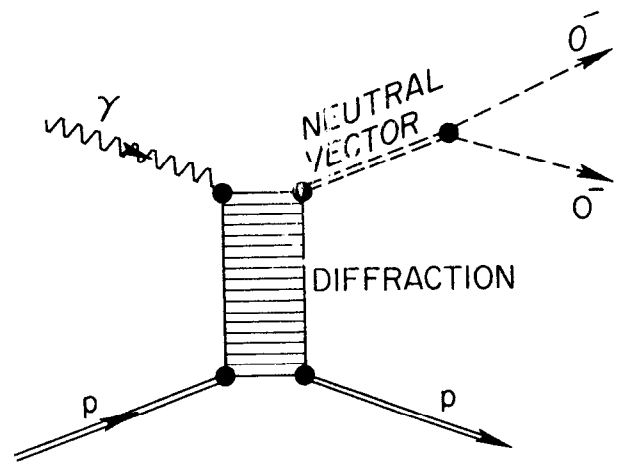
(b)



(c)

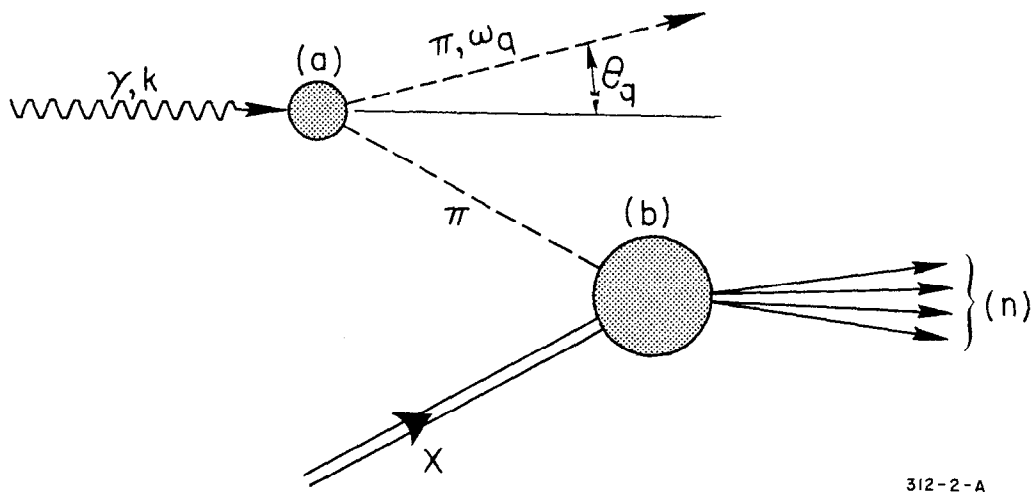


(d)



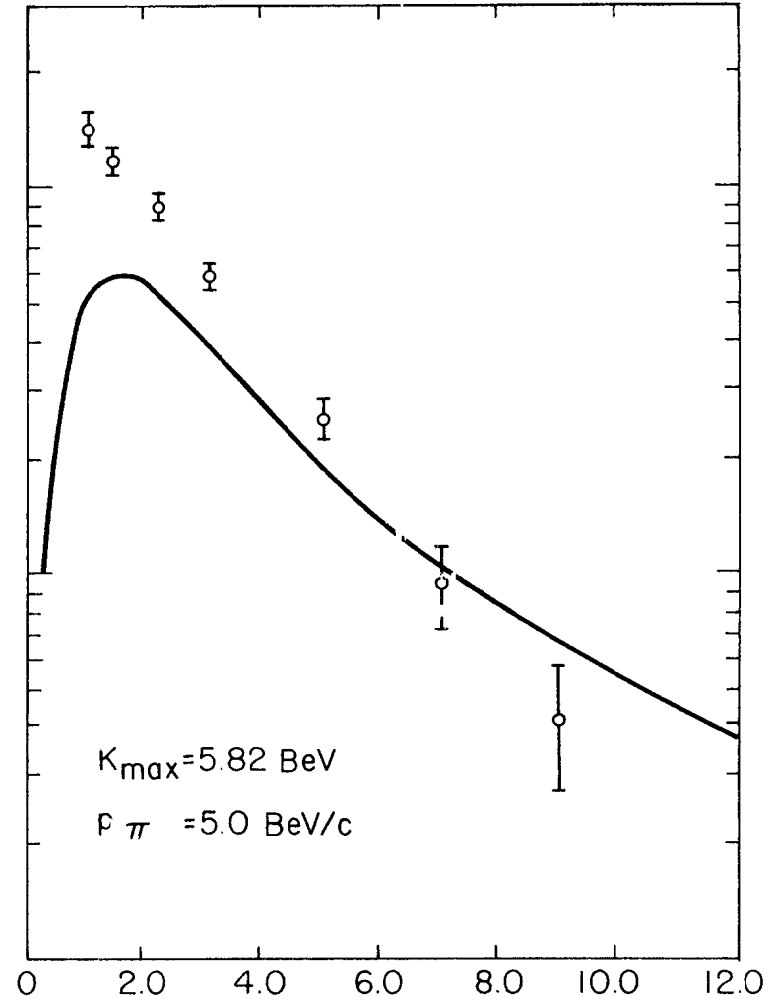
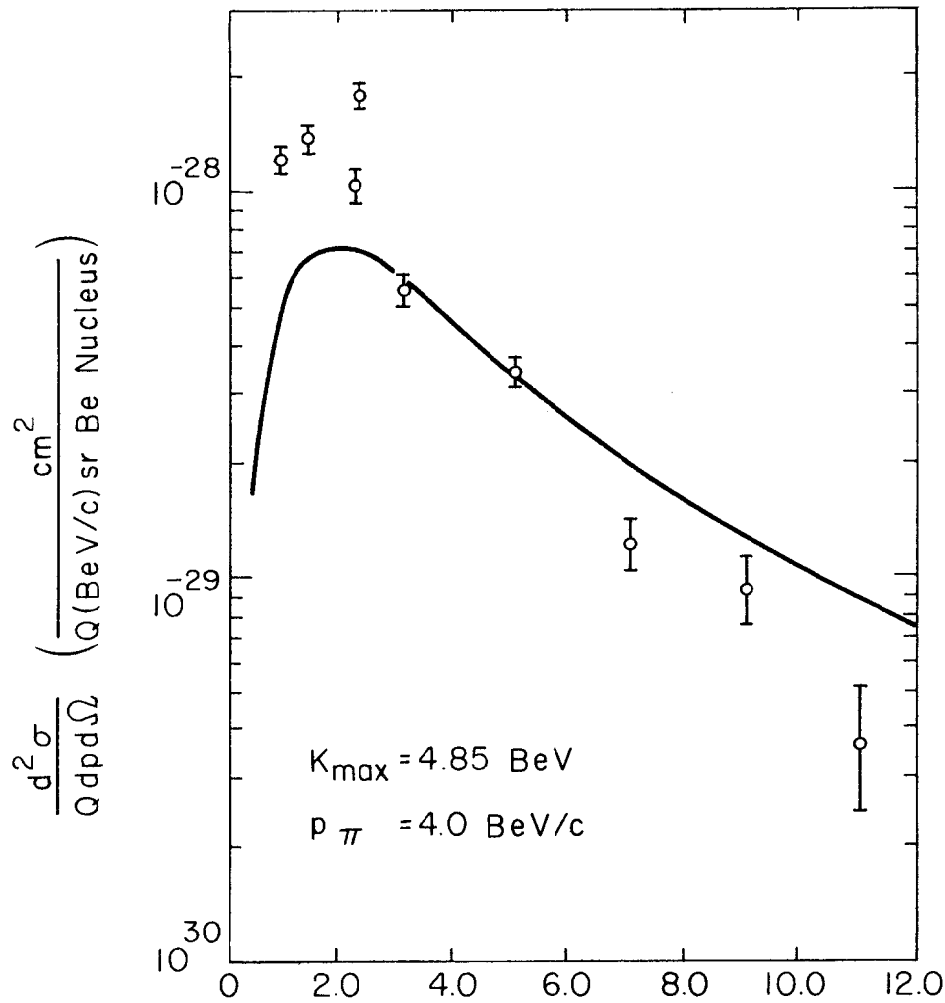
(e)

Fig. 1



312-2-A

Fig. 2



LABORATORY ANGLE IN DEGREES

Fig. 3

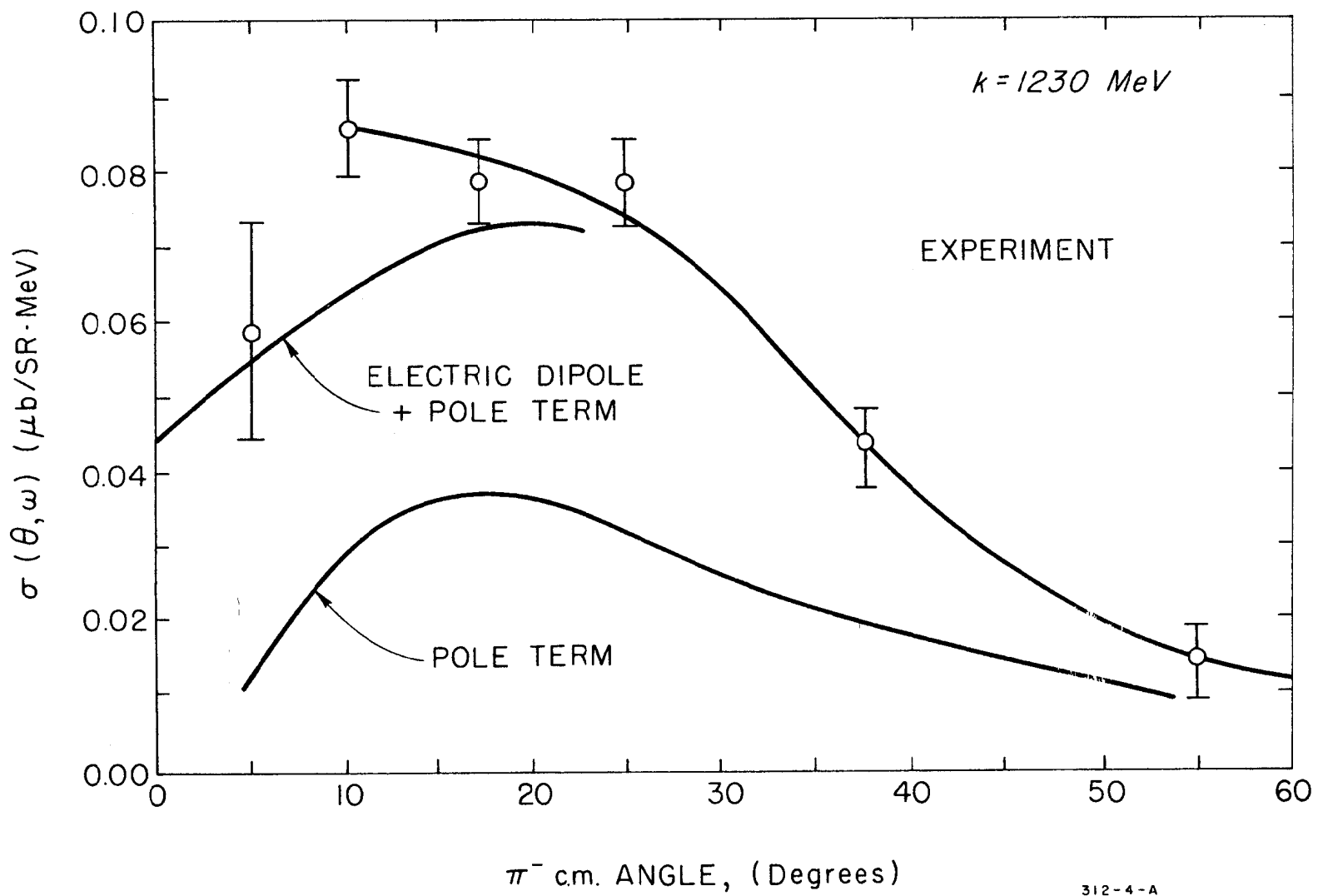
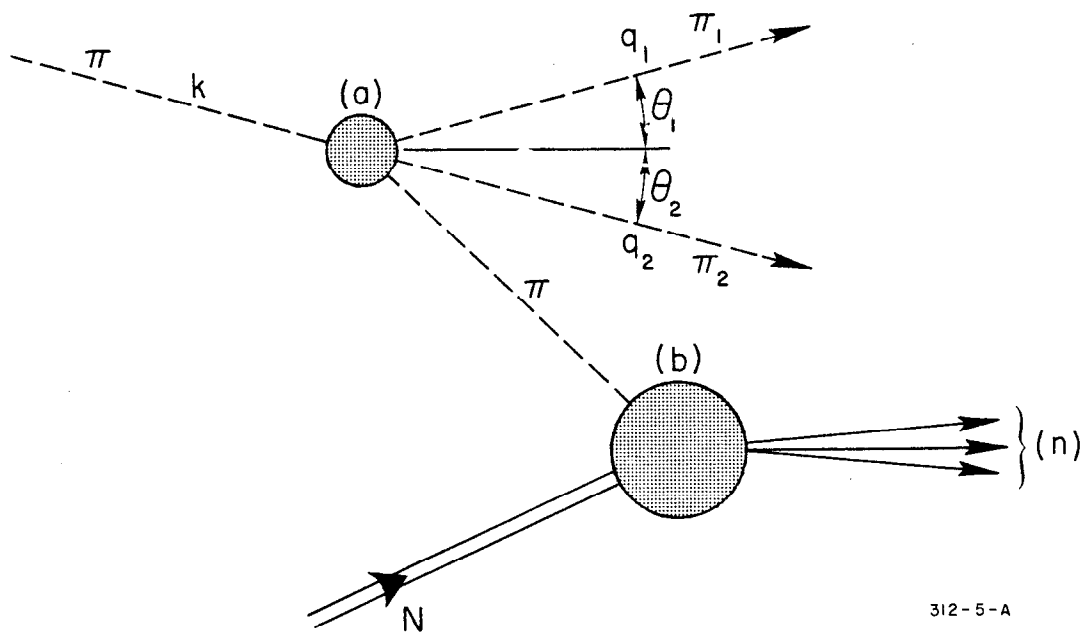


Fig. 4



312-5-A

Fig. 5

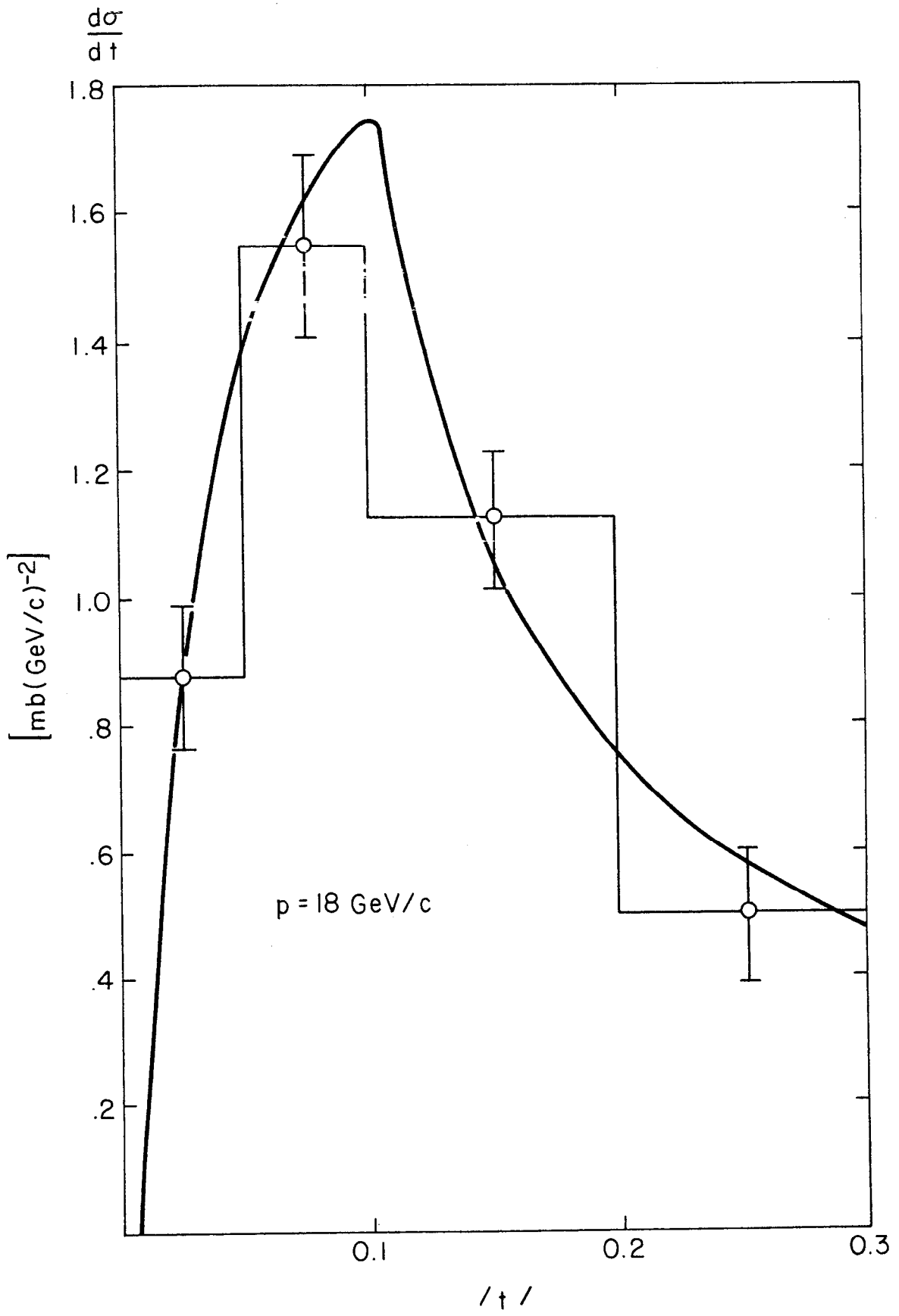


Fig. 6

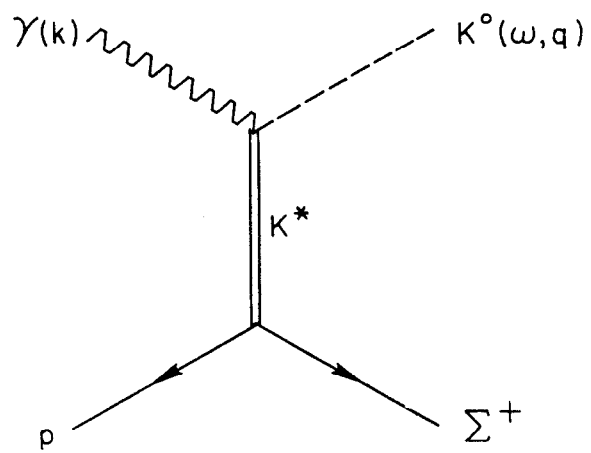


Fig. 7

189-1-A

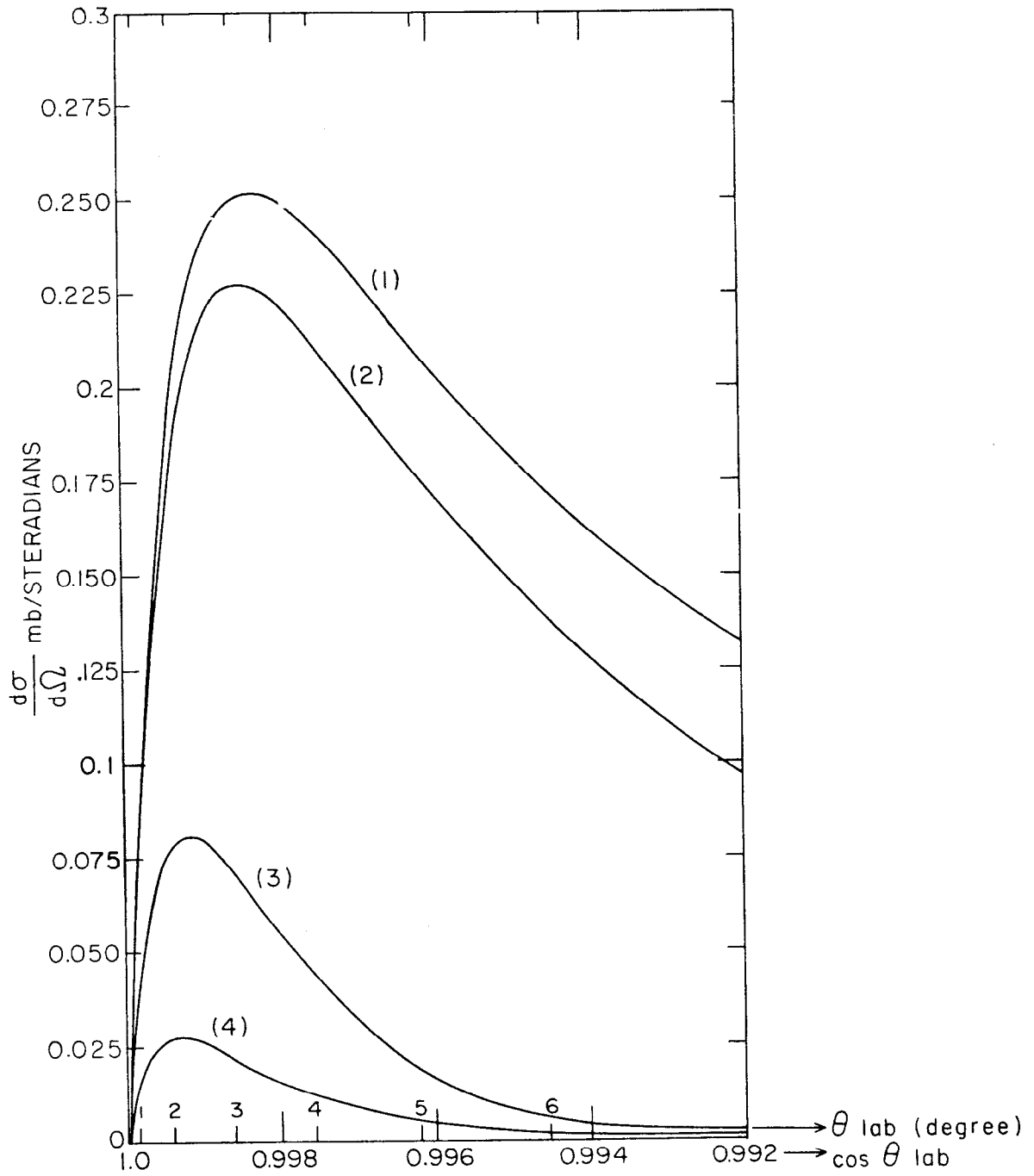


Fig. 8

189-5-A

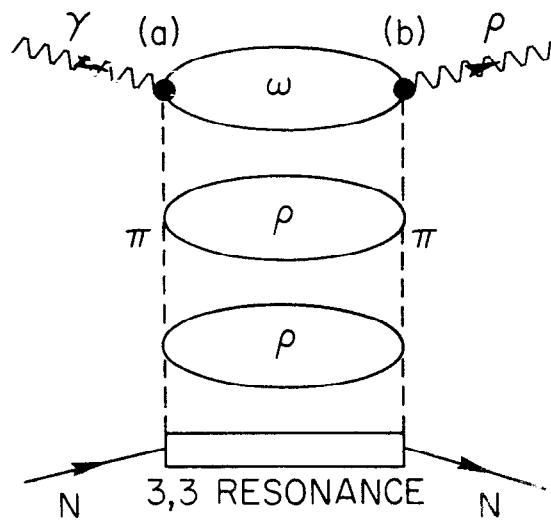
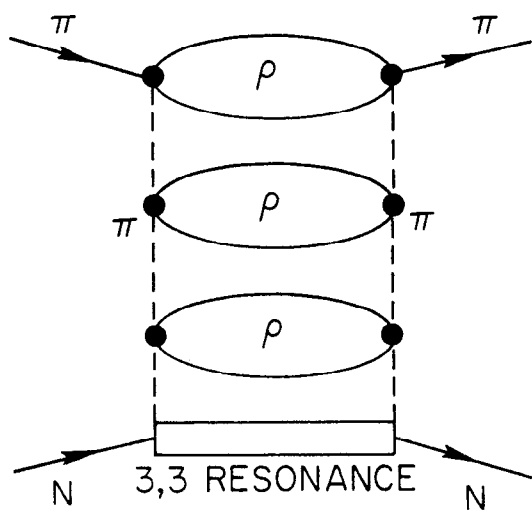
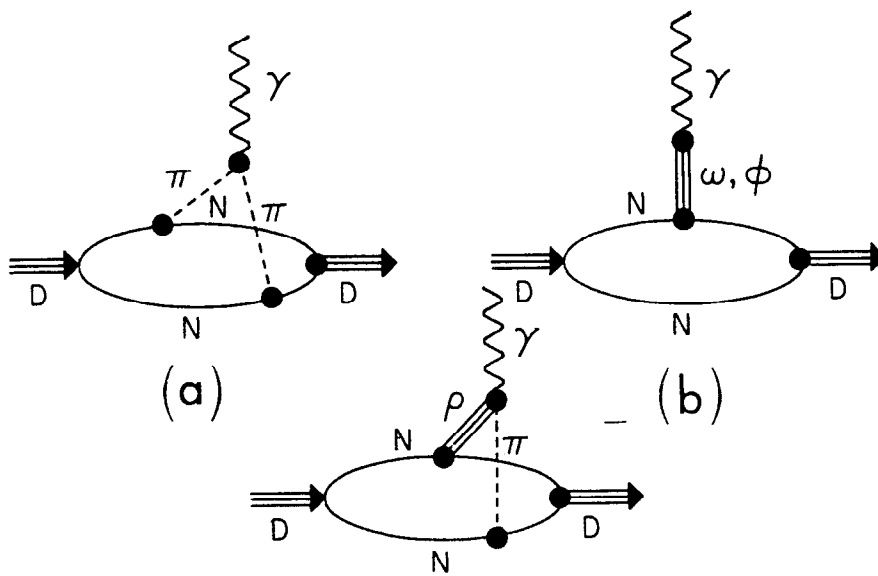
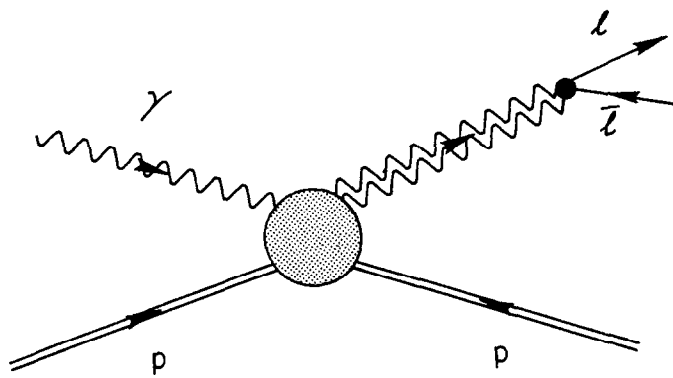


Fig. 9



312-14-A

Fig. 10



312-15-A

Fig. 11

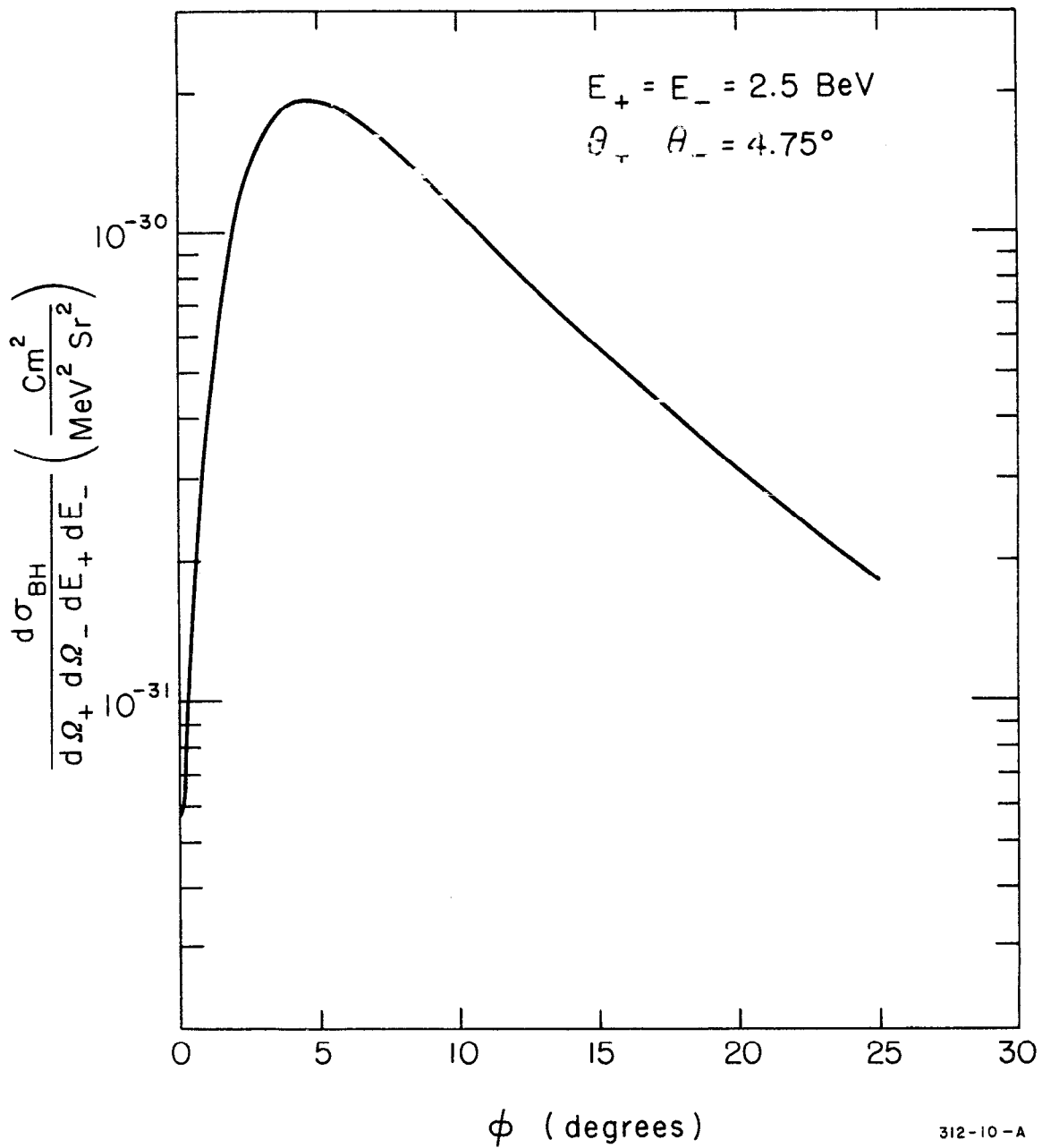


Fig. 12

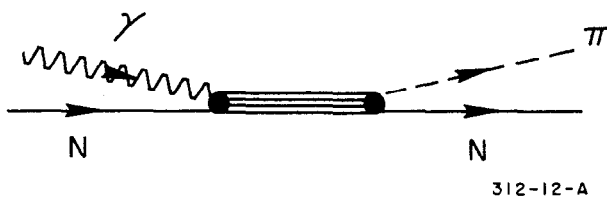


Fig. 13

312-12-A